

UNCLASSIFIED

AD 268 121

*Reproduced
by the*

**ARMED SERVICES TECHNICAL INFORMATION AGENCY
ARLINGTON HALL STATION
ARLINGTON 12, VIRGINIA**



UNCLASSIFIED

NOTICE: When government or other drawings, specifications or other data are used for any purpose other than in connection with a definitely related government procurement operation, the U. S. Government thereby incurs no responsibility, nor any obligation whatsoever; and the fact that the Government may have formulated, furnished, or in any way supplied the said drawings, specifications, or other data is not to be regarded by implication or otherwise as in any manner licensing the holder or any other person or corporation, or conveying any rights or permission to manufacture, use or sell any patented invention that may in any way be related thereto.

Approved by the Chief, Bureau of Ships (Code 535)

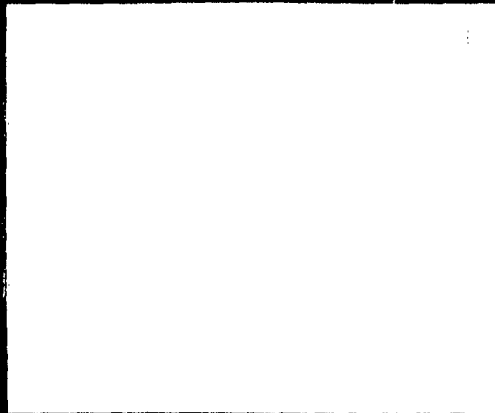
268121

268 121

UNIVERSITY OF CALIFORNIA

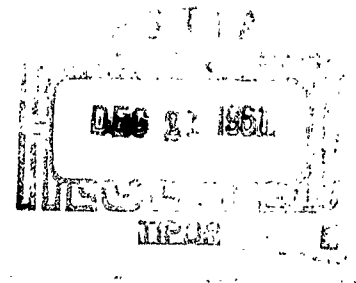
SCRIPPS INSTITUTION OF OCEANOGRAPHY

VISIBILITY LABORATORY



268 121

Visibility Laboratory
University of California
Scripps Institution of Oceanography
San Diego 52, California



THE REDUCTION OF CONTRAST BY ATMOSPHERIC BOIL

S. Q. Duntley, W. H. Culver
F. Richey and R. W. Preisendorfer

72 0 100

1 July 1958
Index Number NS 714-100

Bureau of Ships
Contract NObs-72092

SIO REFERENCE 58-35

Approved:

Seibert Q. Duntley
Seibert Q. Duntley, Director
Visibility Laboratory

Approved for Distribution:

Roger Revelle
Roger Revelle, Director
Scripps Institution of Oceanography

*


THE REDUCTION OF CONTRAST BY ATMOSPHERIC BOIL

**

Seibert Q. Duntley, William H. Culver,
Frances Richey,*** and Rudolph W. Preisendorfer


Scripps Institution of Oceanography, University of California, La Jolla, Calif.

ABSTRACT



It is shown that the probability of receiving light from an object viewed through a turbulent atmosphere follows a normal Gaussian distribution. Furthermore the root mean square angular deflection of the points of any object will be proportional to the square root of the object-to-observer distance.

From relations of the type described in the examples, it is possible to predict the apparent contrast throughout a given scene, provided the inherent contrast distribution, the Optical Air State, and the range of the target is known. The Optical Air State for a given condition of atmosphere can be measured using a telephotometer and a series of long thin black bars of varying widths.



*This paper was prepared under a contract between the University of California and the Bureau of Ships, U. S. Navy. Contribution from The Scripps Institution of Oceanography, University of California, New Series No. _____.

** Present address: Rand Corp., Santa Monica, California

*** Present address: Hughes Aircraft Co., Culver City, California

INTRODUCTION

One of several factors determining the form of the image of a distant object is the time varying distortion caused by inhomogenities in the refractive index of the atmosphere. As is well known, the shimmer of distant objects is caused by spatial and temporal variations in the index of refraction of rising columns of hot air, with the resulting disturbance of the propagated electromagnetic radiation. This disturbance causes time varying distortion of the image and loss of fine detail.

This phenomenon is of particular interest to the geodesist, because it limits the precision with which a telescope can be pointed at a distant object¹, and to the astronomer, because it blurs the images of the stars and limits his resolving power.

Experiments on time varying characteristics of optical transmission through an inhomogeneous atmosphere have been made by Riggs, Mueller, Graham, and Mote², who found that for a path length of several hundred meters the average apparent instantaneous displacement of a point on a target was greater than 3 seconds of arc with a maximum displacement of 9 seconds. The instantaneous displacements of points separated by more than 5 minutes of arc were uncorrelated.

Some of the time varying characteristics of the shimmer effect are slow enough to be discernable to the eye, but much of the effect is so rapid that only time averaged values of the radiance of the image are important for visual observation.

The analytic treatment of the propagation of electromagnetic waves

¹ Washer, F. E., Williams, H. B., "Precision of Telescope Pointing for Outdoor Targets," J. Opt. Soc. Am. 36, 400 (1946).

² Riggs, Mueller, Graham, and Mote, "Photographic Measurements of Atmospheric Boil," J. Opt. Soc. Am. 37, 415 (1947).

through inhomogeneous media has been considered by a large number of investigators. The rigorous solution of the problem by perturbation methods in terms of the statistical parameters of the inhomogeneities yields results in very untractable forms, especially for one interested in the transmission of optical images. Results derived from approximate models have been useful for specific problems. The use of the approximation of geometric optics yields results in a form that are most easily used in problems of optical image transmission, particularly for the consideration of the time-averaged image.

The validity of the geometrical optics approximation of a particular case can be ascertained by the value of the quantity $a^2/\lambda r$ where a is a representative size of a turbulent element, λ is the wave length of light, and r is the distance from the turbulence to the observer. If $a^2/\lambda r \gg 1$ the geometrical optics approximation is valid.³

For a slit of width "a" the size of the diffraction pattern is equal to the geometric image of the slit when $a^2/\lambda r = 1$. Thus the criterion above is seen to be plausible.

The problem of transmission through an inhomogeneous medium has been treated by (using the geometrical optics approximation) Bergmann⁴ and Chandrasekhar⁵. The results of this paper are consistent with some of those of Chandrasekhar but are derived from less restrictive assumptions.

For an investigator interested in image transmission the distortion property of an inhomogeneous medium is usefully described in terms of the distortion of a point source. More precisely, let a given point in the object space be designated by the pair of direction components (ψ'_x, ψ'_y) ,

³ Booker, H. G., and Gordon, W. E., "Outline of a theory of radio scattering in the troposphere," J. Geophys. Res. 55, 241 (1950).

⁴ Bergmann, P. G., "Propagation of radiation in a medium with random inhomogeneities," Phys. Rev. 70, 486 (1946).

⁵ Chandrasekhar, S., "A statistical basis for the theory of stellar scintillation," Monthly Not. Roy. Astron. Soc. 112, 475 (1952).

and let the point be assigned a unit isotropic radiance. The exact form of (ψ'_x, ψ'_y) will be given later. If the distortion action of the medium changes sufficiently rapidly over an interval of time, the successive images (ψ_x, ψ_y) of (ψ'_x, ψ'_y) appear essentially as a continuum of points (a blur) in the image space. For the purposes of this discussion, a function \mathcal{P} is defined which assigns to each object point (ψ'_x, ψ'_y) the time-averaged radiance $\mathcal{P}(\psi_x - \psi'_x, \psi_y - \psi'_y)$ of the image point (ψ_x, ψ_y) . The time-averaged radiance distribution \bar{N} on the image space is then representable as a convolution of the function \mathcal{P} with the radiance distribution N on the object space:

$$\bar{N}(\psi_x, \psi_y) = \int_{\mathcal{V}} N(\psi'_x, \psi'_y) \mathcal{P}(\psi_x - \psi'_x, \psi_y - \psi'_y) d\psi'_x d\psi'_y, \quad (1)$$

where \mathcal{V} is the object space, namely the collection of all directions (ψ'_x, ψ'_y) . Since the location of the observer is held fixed throughout the entire discussion, the location symbol \underline{x} has been suppressed in the radiance function notation (ordinarily written $N(\underline{x}, \psi_x, \psi_y)$).

In the following discussion attention is given to the statistics of the deviations undergone by a ray traversing a path between a point source and a screen some distance away. Because of an optical reciprocity law this derivation applies equally well to an extended field of view, from which light is received by a 'point' receiver such as an eye or a lens.

METHOD OF APPROACH

A theoretical treatment for transmission through any inhomogeneous

medium* has been evolved which is based on the following considerations: The path of sight is assumed to lie within a (spatially and temporally) uniformly turbulent medium made up of uncorrelated optically inhomogeneous regions with dimensions small compared to the distance through which the ray travels. Each light ray undergoes a large number of deflections. Only small angle deflections need be considered. Using only these assumptions we may consider the following.

Figure 1 shows the path of a light ray emitted at P_0 traversing a turbulent medium toward an arbitrarily oriented screen TT' a distance r from the source. The plane of the figure is perpendicular to TT' and passes through the path P_0Q of the undeviated ray. Two perpendicular axes--the x - and y -axis lie in TT' . A segment TQT' of the x -axis is shown. The y -axis is normal to the plane of the figure and goes through Q . The ray now travels from P_0 to a point P_1 determined by the condition that the ray will have turned through an angle whose projection on the plane of the figure is of a small fixed magnitude α (in radians). In accordance with our assumptions, the distance along the segment P_0P_1 is large compared to the dimensions of the centers of turbulence. The projection (in the manner shown in the figure) of P_1 falls on TT' a distance x_1 away from Q . As the ray continues along its path from P_1 it will undergo further deflections. When its direction has been changed through another angle whose projection in the plane of the figure is of the same magnitude α , P_2 is projected on the screen, where it falls a distance x_2 away from the projection of P_1 .

*Including the oceans and other bodies of water, wherein refractive inhomogeneities may result from suspensoids, including transparent planktonic organisms, in addition to any inhomogeneities of the water itself.

In the same way the remainder of the path of the ray is divided up into segments representing equal angles of deviation α , and the projection of each endpoint P_i is mapped onto the screen TT' . Finally x_n will be the x -distance on TT' of the projection of P_n from the projection of P_{n-1} where $P_{n-1}P_n$ is the last such path segment traversed by the ray before it strikes the screen. No generality is lost if P_n is taken to lie on TT' . Since the distance over P_iP_{i+1} is large compared to the dimensions of the centers of turbulence, it follows that the curvature of the ray between P_i and P_{i+1} is uncorrelated with its curvature during its past or future history so that the directions of projected path segments are uncorrelated.

The magnitude of x_i can be found in the following way, using the small angle assumption. If D_i is the distance from P_i to TT' , then $x_i = D_i\alpha$. For a large number n of deflections, the value of D_i will approach an average value given by $(n-i)d_x$, where d_x is the average distance between P_i and P_{i+1} . Then $x_i = (n-i)\alpha d_x$. The algebraic sign associated with any particular x_i has equal probability of being + or -. It can then be seen that the distance from the point Q to the point P_n can be found by summation over all the x_i 's with the appropriate signs.

Because the x_i 's are uncorrelated, they can be considered to be the steps in a one dimensional random walk: Let x_n , the last of the x_i 's be the (signed) length of the first step in the random walk, x_{n-1} the length of the second and so on. Therefore absolute magnitude of the j th step will be $j\alpha d_x, j=1, \dots, n$. The size of the steps in this one dimensional random walk thus increase linearly with each step.

THE DETAILS OF THE DERIVATION

The probability distribution for a one dimensional random walk can be calculated in the following way. The mean square deviation $\sigma^2(n)$ of the distribution for a walk of n steps is **equal** to the sum of the mean square deviations for each step:

$$\sigma^2(n) = \sum_{j=1}^n \sigma_j^2 ,$$

where

$$\sigma_j = j \alpha d_x$$

is the (signed) length of the j th step.

Therefore

$$\sigma^2(n) = \sum_{j=1}^n j^2 \alpha^2 d_x^2 = \alpha^2 d_x^2 \left[\frac{n(n+1)(2n+1)}{6} \right] .$$

For large n the expression in brackets approaches : $n^3/3$.

Therefore

$$\sigma^2(n) = \alpha^2 d_x^2 n^3/3 .$$

From a special central limit theorem due to Liapounoff,⁶ it can be shown that the angular probability distribution approaches a normal distribution whose mean is the position on the screen reached by the undeviated ray. Liapounoff's Theorem states the following: let x_1, x_2, x_3, \dots , be independent random variables, and denote m_j and σ_j as the mean and standard deviation of x_j . Suppose that the third absolute moment of x_j about its mean:

$$\rho_j^3 = \text{Expectation} (|x_j - m_j|^3)$$

⁶ Cramer, H., Mathematical Methods of Statistics (Princeton Univ. Press, 1946), p p. 215-216.

is finite for every j and define ρ^3 as:

$$\rho^3 = \sum_{j=1}^n \rho_j^3.$$

Then if the condition $\lim_{n \rightarrow \infty} [\rho(n)/\sigma(n)] = 0$ is satisfied, the result is that the sum $x = \sum_{j=1}^n x_j$ is asymptotically normal.

This can be applied to the case of the above random walk in the following way:

$$\rho^3(n) = \alpha^3 d_x^3 \sum_{j=1}^n j^3 = \alpha^3 d_x^3 \left[\frac{n^2(n+1)^2}{4} \right].$$

For large n :

$$\rho^3(n) = \alpha^3 d_x^3 n^4 / 4,$$

and,

$$\lim_{n \rightarrow \infty} [\rho(n)/\sigma(n)] = \lim_{n \rightarrow \infty} n^{4/3} / n^{3/2} = \lim_{n \rightarrow \infty} n^{-1/6} = 0,$$

and thus the hypothesis of Liapounoff's theorem is satisfied.

Hence it is shown that a continuum of rays starting with a given initial direction and which traverse a medium whose optical properties are uniformly turbulent will give rise to a continuum of terminal points on the target plane such that the density of the points projected onto the x -axis follows a normal distribution.

Since

$$r = n d_x,$$

we may write alternatively

$$\sigma_x^2(r) = \alpha^2 r^3 / 3 d_x, \quad \text{for fixed } \alpha.$$

Thus the spread of the Gaussian probability distribution increases as the $3/2$ power of r . We now introduce the angular variable $\psi_x \equiv x/r$. In terms of ψ_x , the spread of the probability distribution $P_r(\psi_x)$ is proportional to $r^{1/2}$. The normalized Gaussian probability distribution with root mean square deviation given by

$$\sigma_x(r) = +\sqrt{\frac{\alpha^2 r}{3 \alpha}}$$

is:

$$P_r(\psi_x) = \frac{1}{\sqrt{2\pi} \sigma_x(r)} \exp \left\{ -\frac{1}{2} \left(\frac{\psi_x}{\sigma_x(r)} \right)^2 \right\}.$$

The above derivation may be extended to the two-dimensional case. The new derivation is similar in all details to the former. In particular the same angle α is used. However, the projections of all ray segments are now onto the y -axis in the plane TT' , and in general a new average distance d_y must be introduced. The result is:

$$P_r(\psi_y) = \frac{1}{\sqrt{2\pi} \sigma_y(r)} \exp \left\{ -\frac{1}{2} \left(\frac{\psi_y}{\sigma_y(r)} \right)^2 \right\}, \quad \psi_y \equiv y/r, \quad \sigma_y(r) = \sqrt{\frac{\alpha^2 r}{3 \alpha_y}}$$

In general the two-dimensional probability distribution is of the form:

$$P_r(\psi_x, \psi_y) = \frac{1}{2\pi \sigma_x(r) \sigma_y(r) (1-\rho^2)} \exp \left\{ \frac{-1}{2(1-\rho^2)} \left[\left(\frac{\psi_x}{\sigma_x(r)} \right)^2 - \frac{2\rho \psi_x \psi_y}{\sigma_x(r) \sigma_y(r)} + \left(\frac{\psi_y}{\sigma_y(r)} \right)^2 \right] \right\}$$

where ρ is the correlation coefficient between $P_r(\psi_x)$ and $P_r(\psi_y)$.

Along a horizontal path of sight the vertical displacement of a point would be expected to be uncorrelated with the horizontal displacement. In this case

$$P_r(\psi_x, \psi_y) = \frac{1}{2\pi \sigma_x(r) \sigma_y(r)} \exp \left\{ -\frac{1}{2} \left[\left(\frac{\psi_x}{\sigma_x(r)} \right)^2 + \left(\frac{\psi_y}{\sigma_y(r)} \right)^2 \right] \right\}.$$

If the turbulence is isotropic, i.e., if $d_x = d_y = d$, then

$$\sigma_x(r) = \sigma_y(r) = \sqrt{\frac{\alpha^2 r}{3 \alpha}} = \sigma(r).$$

If we set $\psi^2 = \psi_x^2 + \psi_y^2$, then under these assumptions ($\rho = 0$, $d_x = d_y$) we have

$$P_r(\psi_x, \psi_y) = \frac{1}{2\pi\sigma^2(r)} \exp\left\{-\frac{1}{2}\left(\frac{\psi}{\sigma(r)}\right)^2\right\}.$$

The foregoing formulas give the probability that the terminal point P_n on TT' of a light ray aimed along P_0Q lies in the direction (ψ_x, ψ_y) as seen from P_0 . By tracing the light ray in the opposite direction, these formulas admit the following interpretation: they give the probability that the image of the point (ψ_x, ψ_y) on TT' is at the origin $(0,0)$ of TT' . For fixed r , P_r is thus the required function defined in (1).

OPTICAL AIR STATE

The lower limit on the size of α is determined by the condition that the direction of successive steps be uncorrelated. This condition will be fulfilled if (as assumed above) the average distances d_x and d_y between successive P_i 's is large compared to the dimensions of the inhomogeneities of the medium. It follows that the quantities $A_x = (\alpha^2/3d_x)$ and $A_y = (\alpha^2/3d_y)$ are properties only of the medium and not of the target. The pair of numbers (A_x, A_y) is called the optical air state of the medium and gives a useful measure of the optical turbulence of the atmosphere. If the turbulence is isotropic, the optical air state is a single number $A = A_x = A_y$. In most applications the turbulence is essentially isotropic. The assumptions $\rho = 0$, $A_x = A_y$ will be in force for the remainder of the paper. As a consequence we may write

$$P_r(\psi_x) = \frac{1}{\sqrt{2\pi Ar}} \exp\left\{-\frac{\psi_x^2}{2Ar}\right\},$$

$$P_r(\psi_y) = \frac{1}{\sqrt{2\pi Ar}} \exp\left\{-\frac{\psi_y^2}{2Ar}\right\},$$

and

$$\mathcal{Q}_r(\psi_x, \psi_y) = P_r(\psi_x) P_r(\psi_y) = \frac{1}{2\pi A_r} \exp \left\{ -\frac{\psi^2}{2A_r} \right\} \quad (2)$$

where

$$-\infty < \psi_x < +\infty, \quad -\infty < \psi_y < +\infty, \quad \psi^2 = \psi_x^2 + \psi_y^2.$$

TIME-AVERAGED APPARENT RADIANCE

Actual computations of the time-averaged apparent radiance distribution \bar{N}_r can now be carried out by means of formula (1) in which the explicit expression (2) for the function \mathcal{Q} is used. A particularly useful formula for \bar{N}_r arises in the following special but important context: let a target occupy a subregion \mathcal{V}_t of object space $\mathcal{V} = \{(\psi'_x, \psi'_y) : -\infty < \psi'_x < \infty, -\infty < \psi'_y < \infty\}$; let the apparent radiance distribution N_r over \mathcal{V}_t be uniform and of magnitude ${}_tN_r$. Let the remaining portion \mathcal{V}_b of the object space (the background of the target) have uniform apparent radiance of magnitude ${}_bN_r > 0$. Then, from (1):

$$\begin{aligned} \bar{N}_r &= \int_{\mathcal{V}} N_r \mathcal{Q}_r = \int_{\mathcal{V}_t} N_r \mathcal{Q}_r + \int_{\mathcal{V}_b} N_r \mathcal{Q}_r = \int_{\mathcal{V}_t} {}_tN_r \mathcal{Q}_r + \int_{\mathcal{V}_b} {}_bN_r \mathcal{Q}_r \\ &= ({}_tN_r - {}_bN_r) \int_{\mathcal{V}_t} \mathcal{Q}_r + {}_bN_r. \end{aligned}$$

This result, in more detail, states that

$$\bar{N}_r(\psi_x, \psi_y) = ({}_tN_r - {}_bN_r) \int_{\mathcal{V}_t} \mathcal{Q}_r(\psi_x - \psi'_x, \psi_y - \psi'_y) d\psi'_x d\psi'_y + {}_bN_r \quad (3)$$

for all (ψ_x, ψ_y) in \mathcal{V} .

A perusal of the derivation of \mathcal{Q}_r would show that (3) (and in fact any formula making use of the derived \mathcal{Q}_r) is strictly applicable only to those

regions Ψ_t of Ψ which are angularly small. It is precisely this kind of target, however, which is of primary concern in contrast reduction problems involving atmospheric boil. These targets have their time-averaged radiance greatly influenced by their background radiance. On the other hand, the time-averaged background radiance of such targets is virtually unaffected by the target's radiance.

TIME-AVERAGED APPARENT CONTRAST

The introduction of the notion of contrast greatly facilitates the solution of visibility problems. Let (ψ_x, ψ_y) and (ψ'_x, ψ'_y) be any two points in either image or object space. The contrast $C(\psi_x, \psi_y)$ of (ψ_x, ψ_y) with respect to (ψ'_x, ψ'_y) is defined as

$$C(\psi_x, \psi_y) = [N(\psi_x, \psi_y) - N(\psi'_x, \psi'_y)] / N(\psi'_x, \psi'_y),$$

where N is a given radiance distribution, $N(\psi'_x, \psi'_y) > 0$.

As an example consider the apparent radiance distribution N_r defined in the preceding section. Let (ψ'_x, ψ'_y) be an arbitrary fixed point in Ψ_b . Then the apparent contrast function C_r on Ψ has the following form:

$$C_r(\psi_x, \psi_y) = \begin{cases} C_r & \text{for } (\psi_x, \psi_y) \text{ in } \Psi_t, \\ 0 & \text{for } (\psi_x, \psi_y) \text{ in } \Psi_b. \end{cases} \quad C_r \equiv \frac{(tN_t - bN_t)}{bN_t}$$

In this context we can say that the target Ψ_t has a contrast C_r with respect to its background Ψ_b . In accordance with the general definition of contrast, the time-averaged apparent contrast function \bar{C}_r necessarily has the form:

$$\bar{C}_r(\psi_x, \psi_y) = [\bar{N}_r(\psi_x, \psi_y) - \bar{N}_r(\psi'_x, \psi'_y)] / \bar{N}_r(\psi'_x, \psi'_y).$$

Now let (ψ'_x, ψ'_y) be an arbitrary fixed point in Ψ_b . In view of the comments of the preceding section, we may for all important cases write $\bar{C}_r(\psi_x, \psi_y)$ as:

$$\bar{C}_r(\psi_x, \psi_y) = [\bar{N}_r(\psi_x, \psi_y) - bN_r] / bN_r, \quad (4)$$

where (ψ_x, ψ_y) is any point in Ψ . By adopting this convention (3) yields the following approximate but highly useful contrast formula:

$$\bar{C}_r(\psi_x, \psi_y) = C_r \int_{\Psi_t} Q_r(\psi_x - \psi'_x, \psi_y - \psi'_y) d\psi'_x d\psi'_y \quad (5)$$

From this we immediately deduce the general facts that

$$|\bar{C}_r(\psi_x, \psi_y)| \leq |C_r| \quad \text{for all } (\psi_x, \psi_y) \text{ in } \Psi,$$

and the handy rule of thumb for very small targets of area \mathcal{Q} and arbitrary shape:

$$\bar{C}_r = C_r \frac{\mathcal{Q}}{2\pi A r^3}. \quad (6)$$

This points up among other things an inverse-cube decay of \bar{C}_r with range r . This relation may be used to explain in simple terms the loss of fine detail on targets as the observer-target distance is increased. For by subdividing the given target into sufficiently small elements each of area \mathcal{Q} , (6) will describe the time-averaged contrast of the element against its background consisting of the remainder of the target area. Now while the flux from the element falls off at a rate proportional to r^{-2} , the contrast (and hence the detectability) of the element falls off at a rate proportional to r^{-3} . In short, fine detail on a receding target is lost at a greater rate than the flux from the entire target. As a consequence, the detail on a target is lost from view sooner than the target itself.

Despite the concession to complexity made in (4), the resulting formula (5) faithfully reproduces the main features of the time-averaging affect of atmospheric boil phenomena, as the following examples illustrate.

EXAMPLES

A. Long Straight Edge. Consider an infinitely long straight boundary between two regions of object space each with a distinct uniform apparent radiance (Figure 2). For this example, the target Ψ_t consists of all points (ψ_x, ψ_y) such that $\psi_x \leq 0$. The background Ψ_b is the complementary region of all points (ψ_x, ψ_y) such that $\psi_x > 0$. Ψ_t is assigned the uniform apparent radiance ${}_t N_t$. From (3) with (2):

$$\begin{aligned} \bar{N}_r(\psi_x, \psi_y) &= ({}_t N_t - {}_b N_t) \left[\frac{1}{2\pi A_t} \int_{-\infty}^0 \int_{-\infty}^{\infty} \exp \left\{ -\frac{1}{2} \frac{(\psi_x - \psi'_x)^2 + (\psi_y - \psi'_y)^2}{A_t} \right\} d\psi'_x d\psi'_y \right] + {}_b N_t \\ &= ({}_t N_t - {}_b N_t) \left[\frac{1}{\sqrt{2\pi A_t}} \int_{\psi_x}^{\infty} \exp \left\{ -\frac{\psi'^2_x}{2A_t} \right\} d\psi'_x \right] + {}_b N_t . \end{aligned}$$

\bar{N}_r is plotted in Figure 2.

The time averaged apparent contrast is, by (5):

$$\bar{C}_r(\psi_x, \psi_y) = \frac{C_t}{\sqrt{2\pi A_t}} \int_{\psi_x}^{\infty} \exp \left\{ -\frac{\psi'^2_x}{2A_t} \right\} d\psi'_x .$$

The limits

$$\lim_{\psi_x \rightarrow \infty} \bar{C}_r(\psi_x, \psi_y) = 0 ,$$

$$\lim_{\psi_x \rightarrow -\infty} \bar{C}_r(\psi_x, \psi_y) = C_t ,$$

which hold for all ψ_y , agree with the values one would expect on the basis of the values of the unshimmered contrast C_t discussed in the preceding action.

B. Long Thin Bar. A long thin bar may be represented by the sub-region Ψ_t of Ψ consisting of all points (ψ_x, ψ_y) such that $-a \leq \psi_x \leq a$. All other points of Ψ form the background Ψ_b . Ψ_t is assigned the uniform radiance $t N_t$; Ψ_b , the radiance $b N_t$. Then from (5) with (2):

$$\begin{aligned}\bar{C}_r(\psi_x, \psi_y) &= \frac{C_r}{2\pi A_t} \int_{-a}^a \int_{-\infty}^{\infty} \exp \left\{ -\frac{1}{2} \frac{(\psi_x - \psi'_x)^2 + (\psi_y - \psi'_y)^2}{A_t} \right\} d\psi'_x d\psi'_y \\ &= \frac{C_r}{\sqrt{2\pi A_t}} \int_{\psi_x - a}^{\psi_x + a} \exp \left\{ -\frac{\psi'^2_x}{2A_t} \right\} d\psi'_x.\end{aligned}$$

It is easy to verify that $|\bar{C}_r|$ attains a maximum at the point (0,0).

$\bar{C}_r(0,0)$ is the extreme contrast attained by \bar{C}_r over Ψ , i.e., $\bar{C}_r(0,0)$ is either a maximum (if $\bar{C}_r(0,0)$ is positive) or a minimum (if $\bar{C}_r(0,0)$ is negative).

It is clear from the geometry in this and the preceding example that \bar{C}_r is independent of ψ_y . Some contrast profiles of shimmered bars are shown in Figure 5. Observe that the widths of the bars are given in terms of the dimensionless parameter $\sqrt{A_t}$. These facts will be of some use in the discussion of the measurement of A.

C. Rectangle. A rectangle in Ψ centered on the origin is defined as the subregion Ψ_t consisting of all points (ψ_x, ψ_y) such that $-a \leq \psi_x \leq a$, $-b \leq \psi_y \leq b$. From (5) with (2), after some reductions,

$$\bar{C}_r(\psi_x, \psi_y) = \frac{C_r}{2\pi A_t} \left[\int_{\psi_x - a}^{\psi_x + a} \exp \left\{ -\frac{\psi'^2_x}{2A_t} \right\} d\psi'_x \right] \left[\int_{\psi_y - b}^{\psi_y + b} \exp \left\{ -\frac{\psi'^2_y}{2A_t} \right\} d\psi'_y \right].$$

The computations of \bar{C}_r for a rectangle can therefore be carried out by using the results of example B.

D. Circular Disk. A circular disk Ψ_t in Ψ centered on the origin and of angular radius ψ is the set of all points (ψ_x, ψ_y) such that $\psi_x^2 + \psi_y^2 \leq \psi^2$ (Figure 3). From (5) with (2) the associated contrast expression is:

$$\bar{C}_t(\psi_x, \psi_y) = \frac{C_t}{2\pi A_t} \iint_{\psi_x'^2 + \psi_y'^2 \leq \psi^2} \exp \left\{ -\frac{1}{2} \frac{(\psi_x - \psi_x')^2 + (\psi_y - \psi_y')^2}{A_t} \right\} d\psi_x' d\psi_y'.$$

An examination of the function \bar{C}_t would show that in this case $\bar{C}_t([\psi_x^2 + \psi_y^2]^{1/2}, 0) = \bar{C}_t(\psi_x, \psi_y)$ (circular symmetry). It is therefore sufficient to consider the evaluation of

$$\bar{C}_t(\psi_x, 0) = \frac{C_t}{2\pi A_t} \iint_{\psi_x'^2 + \psi_y'^2 \leq \psi^2} \exp \left\{ -\frac{1}{2} \frac{(\psi_x - \psi_x')^2 + \psi_y'^2}{A_t} \right\} d\psi_x' d\psi_y'$$

Adopting the following transformation of coordinates: $\psi_x' = \psi' \cos \theta'$, $\psi_y' = \psi' \sin \theta'$,

we have:

$$\bar{C}_t(\psi_x, 0) = \frac{C_t}{2\pi A_t} \int_0^\psi \exp \left\{ -\frac{(\psi'^2 + \psi_x^2)}{2A_t} \right\} \left[\int_0^{2\pi} \exp \left\{ \frac{\psi' \psi_x \cos \theta'}{A_t} \right\} d\theta' \right] \psi' d\psi'.$$

The inner integral is readily evaluated:

$$\int_0^{2\pi} \exp \left\{ z \cos \theta' \right\} d\theta' = 2 \int_0^\pi \cos(\lambda z \sin \theta') d\theta' = 2\pi I_0(z), \quad z = \frac{\psi' \psi_x}{A_t},$$

where I_0 is a modified Bessel function of the first kind, of zero order, which has the series representation:

$$I_0(z) = \sum_{k=0}^{\infty} \frac{\left(\frac{z}{2}\right)^{2k}}{(k!)^2}.$$

Hence

$$\bar{C}_r(\psi_x, 0) = \frac{C_r}{A_r} \int_0^\psi \left[\sum_{k=0}^{\infty} \frac{\left(\frac{\psi' \psi_x}{2A_r} \right)^{2k}}{(k!)^2} \right] \exp \left\{ -\frac{(\psi'^2 + \psi_x^2)}{2A_r} \right\} \psi' d\psi',$$

which may be rewritten as:

$$\bar{C}_r(\psi_x, 0) = C_r e^{-\phi_x} \sum_{k=0}^{\infty} \frac{\phi_x^k}{(k!)^2} \Gamma(\phi; k+1),$$

where $\Gamma(a; k+1) = \int_0^a y^k e^{-y} dy$ defines the incomplete Gamma function, for which tabulations exist⁷, and $\phi_x = \psi_x^2/2A_r$, $\phi = \psi^2/2A_r$. It is easy to check that $|\bar{C}_r|$ is a decreasing function for increasing ψ_x , so that $|\bar{C}_r|$ attains a maximum at (0,0). Thus if $|\bar{C}_r(0,0)|$ is below a threshold contrast, the entire disk is undetectable. The formula for $\bar{C}_r(0,0)$ is readily obtained:

$$\bar{C}_r(0,0) = C_r \Gamma(\psi^2/2A_r; 1) = C_r (1 - e^{-\psi^2/2A_r}).$$

For angularly small disks

$$\bar{C}_r(0,0) = C_r \frac{Q}{2\pi A_r^3},$$

where $Q = \pi(\psi_r)^2$, and which agrees with (6). If $\psi = \infty$, i.e., if the disk is infinitely large, then since $\Gamma(\infty; k+1) = k!$, the general expression yields:

$$\bar{C}_r(\psi_x, \psi_y) = C_r e^{-\phi_x} \sum_{k=0}^{\infty} \frac{\phi_x^k}{(k!)^2} = C_r,$$

as expected.

E. One example of the effect of atmospheric boil on the ability to resolve two objects which are close together is illustrated in Figure 4. Two identical black bars of angular width $\sqrt{A_r}$, separated an angular distance $2\sqrt{A_r}$, have their contrast profiles smeared into a characteristic shape

⁷. Pearson, Karl, Tables of the Incomplete Gamma function (Camb. Univ. Press, 1946).

shown by the dashed curve. The object space contrast of -1 at the center of each bar is invariably raised to - 0.6 in the image space, and the zero contrast at the center of the gap between the bars is invariably pulled down to - 0.74. Such predictable features of shimmered contrast profiles can be used to generate an experimental procedure for determining A, one of which is appended below.

MEASUREMENT OF OPTICAL AIR STATE

For a bar whose width $2a$ is less than $5\sqrt{Ar}$, the values $|\bar{C}_r(\psi_x, \psi_y)|$ are measurably less than $|\bar{C}_r|$. Figure 5 depicts the contrast profiles of four long black bars (hence $C_r = -1$). The width of each differs by a factor of four from its predecessor. From example B,

$$\bar{C}_r(0,0) = \frac{-1}{\sqrt{2\pi}} \int_{-\frac{a}{\sqrt{Ar}}}^{\frac{a}{\sqrt{Ar}}} e^{-\frac{1}{2}t^2} dt.$$

By means of this integral, each choice of the ratio $2a/\sqrt{Ar}$ leads to a corresponding value $\bar{C}_r(0,0)$. These correspondences are graphed in Figure 6. The experimental procedure consists in measuring $\bar{C}_r(0,0)$ for each bar by scanning the bar with a telephotometer at a given range r . The four corresponding values of $2a/\sqrt{Ar}$ are then picked from the graph. Since r is fixed, and $2a$ is known for each bar, A can then be determined.

We observe finally that before using the graph in Figure 6 the measured values $\bar{C}_r(0,0)$ must be corrected to remove the reduction effect on the contrast induced by the scattering and absorption mechanisms of the atmosphere. For horizontal paths of sight, with the usual uniformity properties, the corrected values are given by $\bar{C}_r(0,0) \exp\{+r/L\}$ where L is the attenuation length of the atmosphere.

Acknowledgment

The authors wish to acknowledge the contributions made by Mr. T. A. Magness of the Marine Physical Laboratory of the Scripps Institution of Oceanography.

CAPTIONS

- Figure 1. Illustrating the geometry of the derivation of \bar{P} .
- Figure 2. Illustrating the time-averaged radiance profile of a shimmered edge (Example A).
- Figure 3. Diagram for the derivation in example D.
- Figure 4. The characteristic shape of the time-averaged contrast profile of two long black bars of the dimensions shown.
- Figure 5. Illustrating the characteristic time-averaged contrast profiles of long black bars as a function of bar-width.
- Figure 6. Graph used in the experimental determination of A.

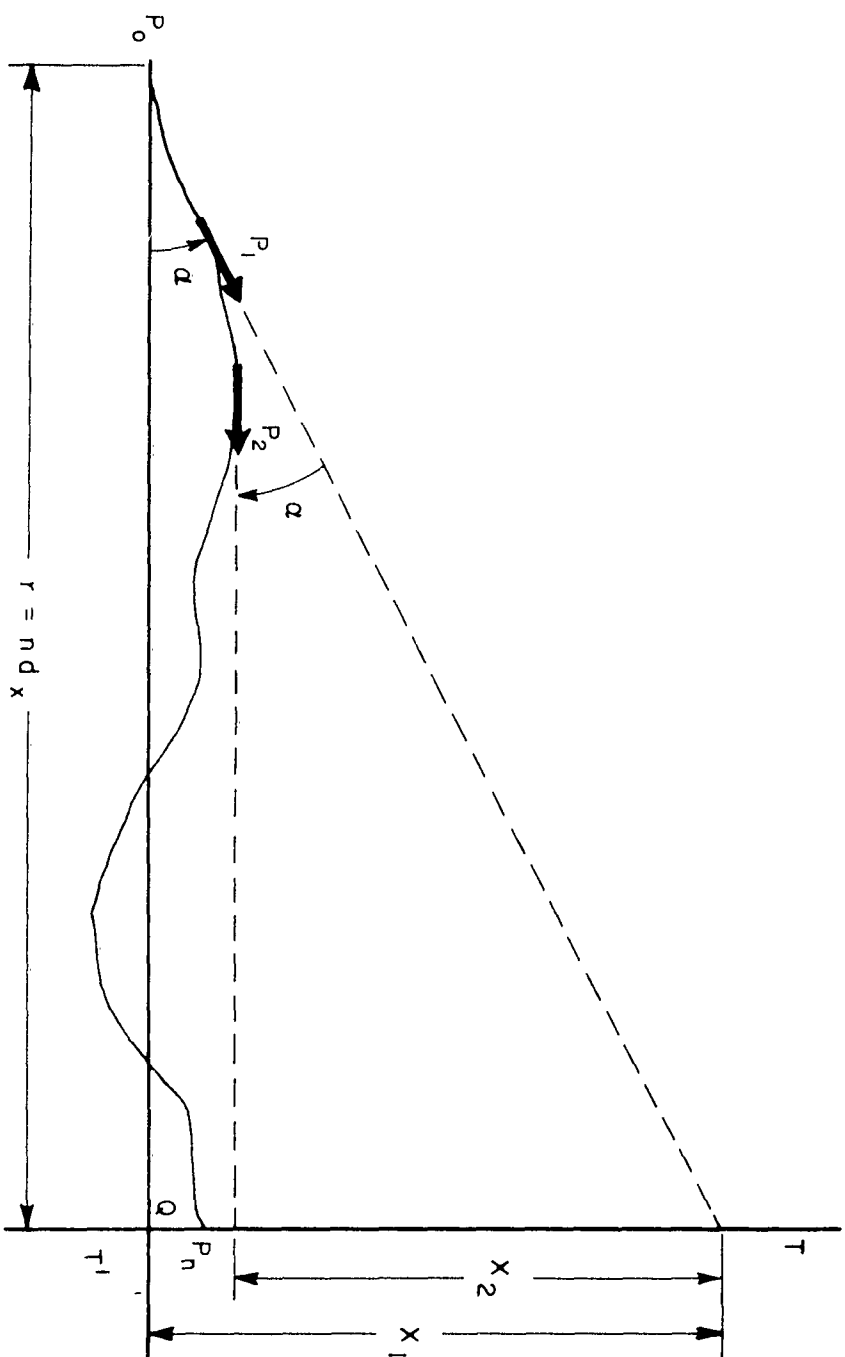


Figure 1
Duntley, Culver, Richey, Preisdorfer

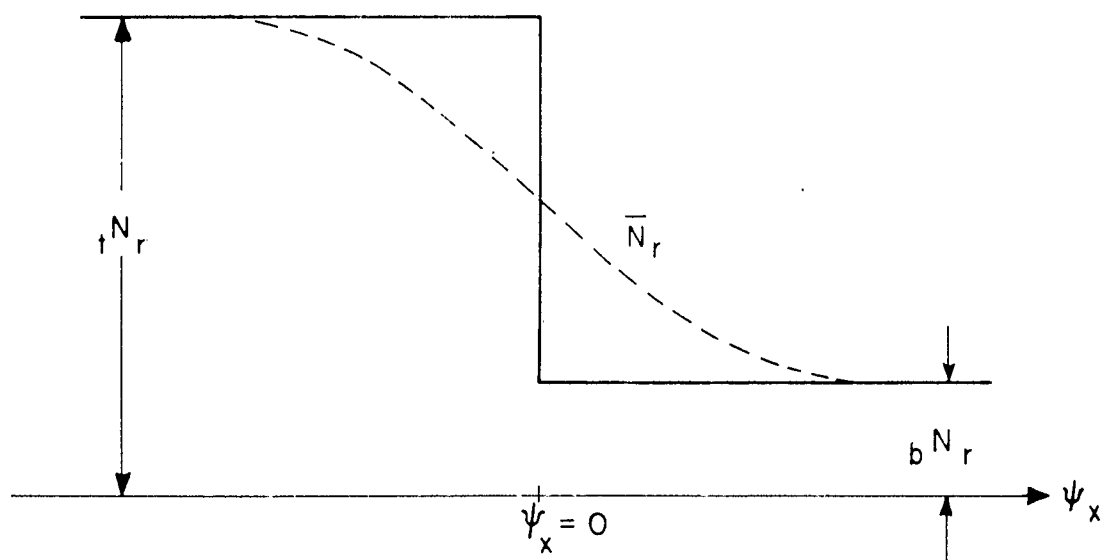


Figure 2
Duntley, Culver, Richey, Preisendorfer

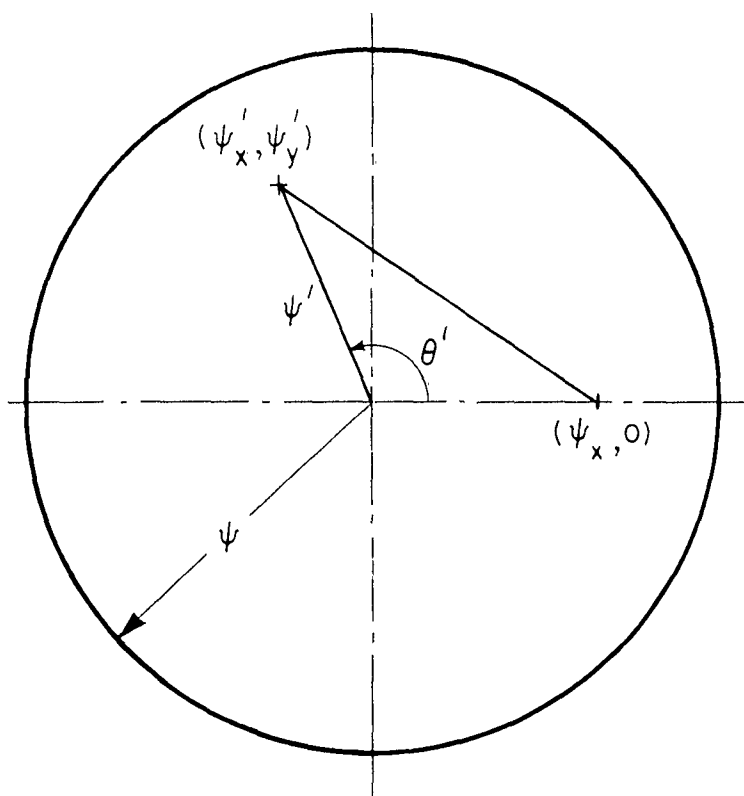


Figure 3
Duntley, Culver, Richey, Preisendorfer

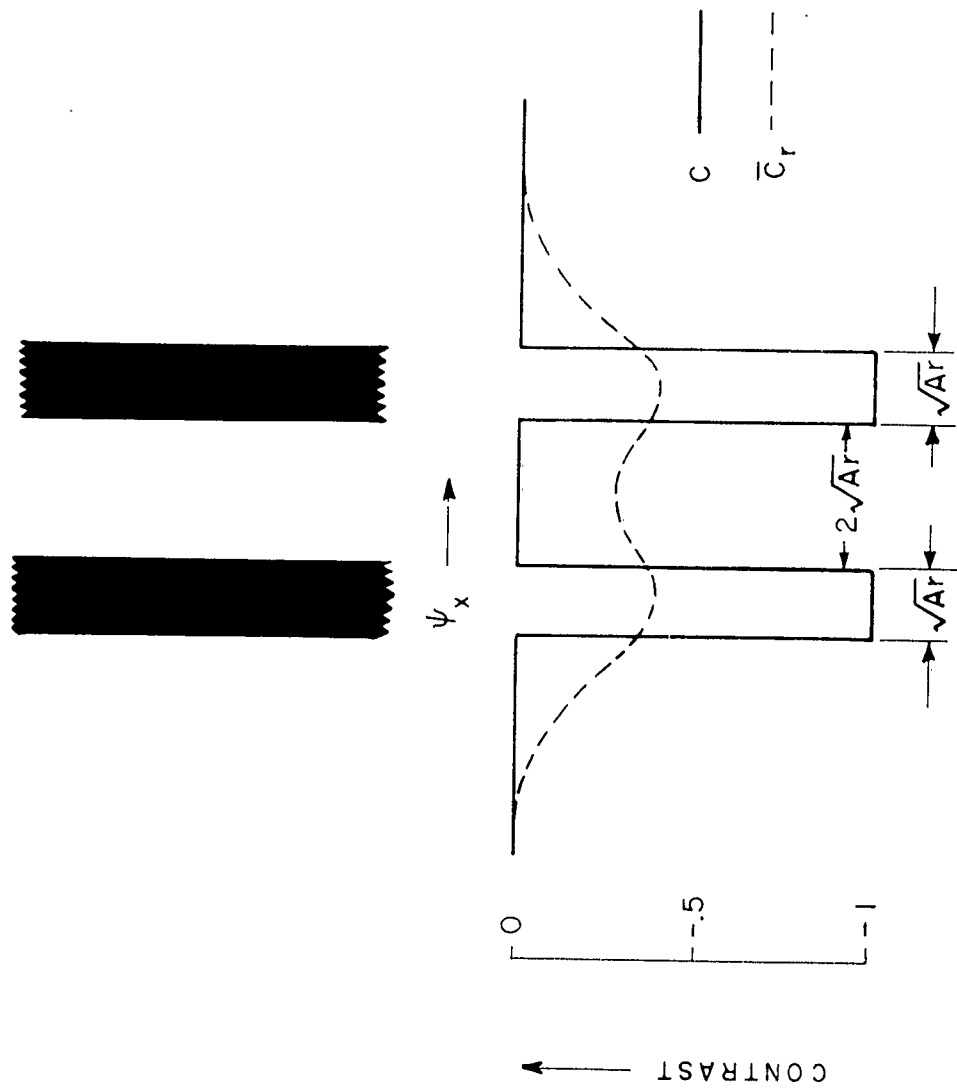


Figure 4
Duntley, Culver, Richey, Preisendorfer

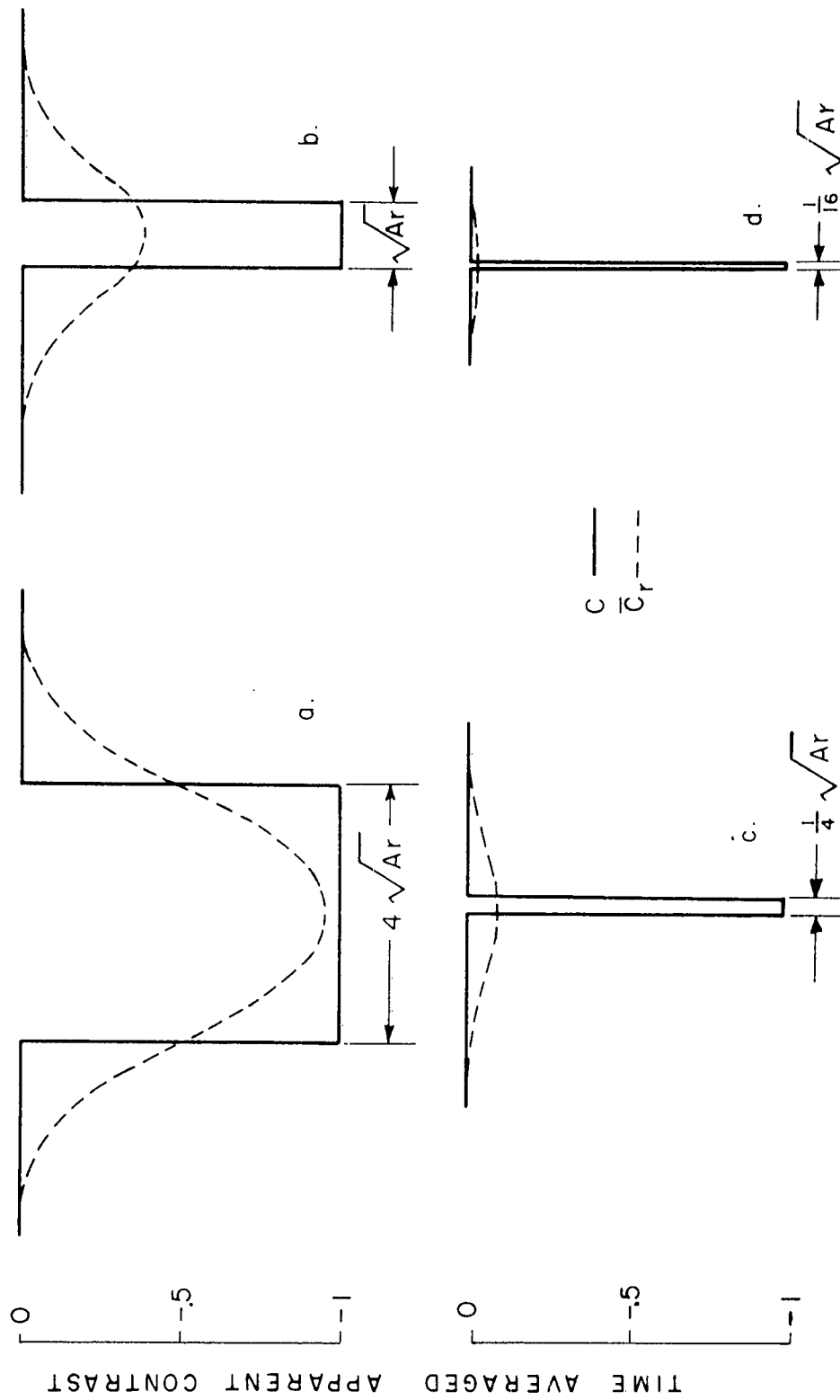


Figure 5
Duntley, Culver, Richey, Preisendorfer

Figure 6
Duntley, Culver, Richey, Preisendorfer

